

Time Evidence Fusion Network: Multi-source View in Long-Term Time Series Forecasting

Tianxiang Zhan

University of Electronic Science and Technology of China
Chengdu, China
ztxtech@std.uestc.edu.cn

Yong Deng*

University of Electronic Science and Technology of China
Chengdu, China
dengentropy@uestc.edu.cn

Yuanpeng He

Peking University
Beijing, China
heyuanpeng@stu.pku.edu.cn

Zhen Li

China Mobile
Beijing, China
zhen.li@pku.edu.cn

ABSTRACT

In practical scenarios, time series forecasting necessitates timeliness, especially when dealing with large datasets. Consequently, the exploration of model architectures remains a perennially trending topic in research. To meet these performance demands, we propose a novel backbone from the perspective of information fusion. Introducing the Basic Probability Assignment (BPA) Module and the Time Evidence Fusion Network (TEFN), based on evidence theory, allows us to achieve superior performance. On the other hand, the perspective of multi-source information fusion effectively improves the accuracy of forecasting. Due to the fact that BPA is generated by fuzzy theory, TEFN also has considerable interpretability. In real data experiments, the TEFN partially achieved state-of-the-art, with low errors comparable to PatchTST, and operating efficiency surpass performance models such as Dlinear. Meanwhile, TEFN has high robustness and small error fluctuations in the random hyperparameter selection. TEFN is not a model that achieves the ultimate in single aspect, but a model that balances performance, accuracy, stability, and interpretability.

PVLDB Reference Format:

Tianxiang Zhan, Yuanpeng He, Yong Deng, and Zhen Li. Time Evidence Fusion Network: Multi-source View in Long-Term Time Series Forecasting. PVLDB, 14(1): XXX-XXX, 2020.
doi:XX.XX/XXX.XX

PVLDB Artifact Availability:

The source code, data, and/or other artifacts have been made available at <https://github.com/ztxtech/Time-Evidence-Fusion-Network>.

1 INTRODUCTION

The evolution of various phenomena is inherently tied to the progression of time, leading to an increasing prevalence of time series data in a multitude of application domains. From health diagnostics,

where the progression of diseases is tracked over time, to financial analysis, where market trends are monitored for investment strategies, and weather forecasting, where atmospheric changes are predicted to safeguard communities, the importance of time series forecasting cannot be overstated. However, as the volume of data grows exponentially, time series forecasting faces significant performance challenges. The sheer scale of big data necessitates more efficient and faster algorithms to process and predict within acceptable time frames, which has become a pressing issue in the field.

In response to these challenges, researchers have been focusing on optimizing the structure of the backbone models used in time series forecasting. It has been observed that linear-based models, such as Dlinear [22], often exhibit superior performance compared to transformer-based models like Crossformer [25], particularly in terms of computational efficiency and speed. These findings highlight the potential of structural optimizations in enhancing the capabilities of time series forecasting models. Nevertheless, the quest for an ideal model that balances performance, prediction accuracy, stability, and interpretability continues. The aim is to develop a model that can provide robust support for high-stakes scenarios where timely and reliable predictions are critical, thereby bridging the gap between theoretical advancements and practical application needs.

Evidence theory, also known as Dempster-Shafer theory, provides a mathematical framework for representing and combining degrees of belief in the presence of uncertainty [6, 17]. It is particularly useful in situations where information is incomplete, ambiguous, or comes from diverse sources. The theory is grounded in the concept of a belief function, which quantifies the degree to which a hypothesis is supported by the available evidence, without necessarily committing to a probability distribution over the possible outcomes. One of the key strengths of evidence theory is its ability to handle the fusion of multiple information sources effectively. This makes it a powerful tool in fields such as data fusion, sensor networks, and multi-criteria decision-making, where diverse pieces of information need to be integrated to form a coherent union. In the realm of symbolic logic, evidence theory often appears as a reasoning framework that offers high interpretability. Unlike traditional probability theory, which requires precise probability assignments, evidence theory allows for a more nuanced representation of uncertainty. It does this through the use of belief

*Corresponding Author

This work is licensed under the Creative Commons BY-NC-ND 4.0 International License. Visit <https://creativecommons.org/licenses/by-nc-nd/4.0/> to view a copy of this license. For any use beyond those covered by this license, obtain permission by emailing info@vldb.org. Copyright is held by the owner/author(s). Publication rights licensed to the VLDB Endowment.

Proceedings of the VLDB Endowment, Vol. 14, No. 1 ISSN 2150-8097.
doi:XX.XX/XXX.XX

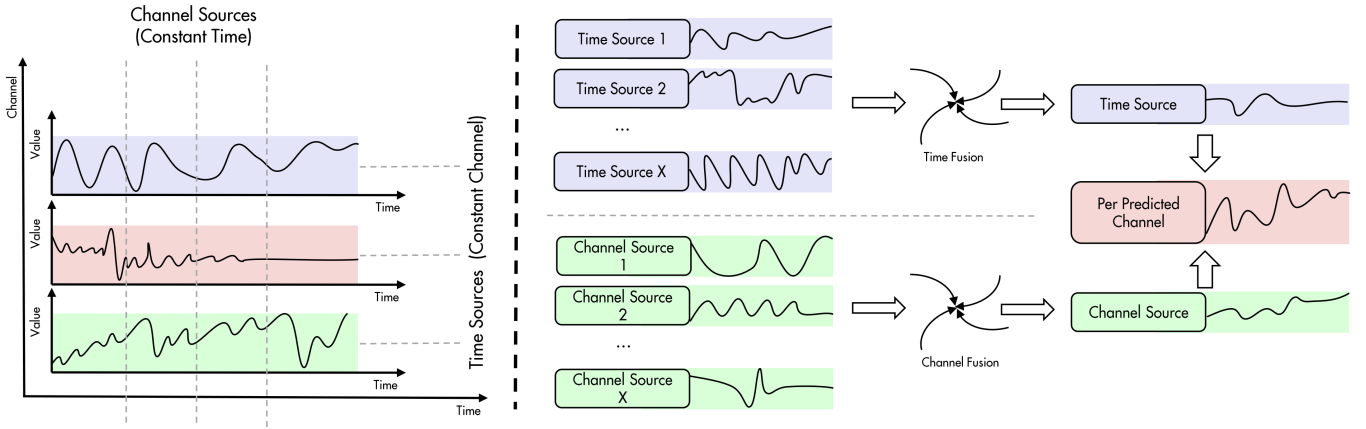


Figure 1: The channel dimension and time dimension of multivariate time series can be considered as different sources of information. Firstly, merge information sources of the same type, and finally integrate information sources from both channel and time dimensions to complete the final prediction.

and plausibility measures, which provide a range of values for the likelihood of an event occurring, rather than a single probability. An innovative application of evidence theory in machine learning is the development of evidence neural networks by Denoeux [8]. These networks are designed for classification tasks and integrate the principles of evidence theory into the architecture of neural networks. By doing so, they enhance the network’s ability to handle uncertainty and provide a more robust and interpretable decision-making process. The evidence neural networks output belief masses that can be directly interpreted as measures of evidence supporting each class, thus offering a clear understanding of the network’s reasoning process.

Therefore, we introduce the Time Evidence Fusion Network (TEFN), a novel architecture designed specifically for regression tasks within the realm of time series forecasting. The conceptual underpinning of TEFN is the innovative strategy of dissecting the time series data into dual perspectives—time and channels—thereby treating each channel and temporal instance as a distinct and autonomous source of information. This approach allows us to leverage the principles of evidence theory to fuse these diverse information streams within an integrated framework, aiming to enhance the accuracy and reliability of predictions as depicted in Figure 1. In essence, TEFN is built upon the premise of simplicity and naïvety in its design philosophy. It refrains from incorporating complex technical modifications that often render models opaque and difficult to interpret. Instead, TEFN maintains a straightforward structure that prioritizes clarity and ease of understanding, making it a transparent and accessible backbone for time series analysis. By adopting this minimalist approach, TEFN emerges as a refreshing alternative in the field, offering a new foundation upon which more sophisticated forecasting models can potentially be built, while retaining the interpretability and trustworthiness that are hallmarks of evidence theory.

In the architecture of TEFN, we introduce a pivotal component termed the Basic Probability Assignment (BPA) Module, which stands as the core of our evidence-theoretic approach to time series

forecasting. The BPA Module operates on the fundamental principles of evidence theory, meticulously mapping various sources of information into mass distributions that are intrinsically linked to the desired target outcome. This mapping is achieved through the application of fuzzy membership functions, which assign membership grades to different fuzzy sets, thereby constructing a comprehensive target distribution as proposed by Deng [7]. In contrast to the convolutional operations prevalent in image processing, which selectively condense features pertinent to the target through filters [4], the BPA Module embodies an expansionary process, as illustrated in Figure 2. Rather than narrowing down to specific features, BPA embraces an expansive perspective, contemplating all potentialities within the event space, which is a collection of subsets derived from the sample space. This expansion across various events is particularly advantageous for the simplistic structures inherent in time series data, enabling a thorough exploration of the myriad hidden informational layers within. For the diverse distributions yielded by the multitude of information sources, we treat each source as an individual sample, and by amalgamating these samples, we utilize the expected forecasting values as the ultimate prediction, thereby delivering a robust and informed forecast that encapsulates the collective wisdom of all contributing sources.

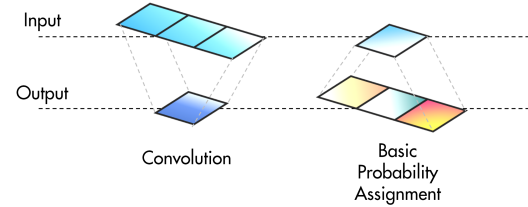


Figure 2: Comparison between convolution and basic probability assignment: convolution condenses information while basic probability assignment diverges to consider different possibilities.

In this paper, we delve into the practical nuances of the Time Evidence Fusion Network (TEFN), examining its precision, memory consumption, training velocity, sensitivity to parameters, and interpretability. To maintain equitable comparisons, all experimental data and configuration files are sourced from open-source initiatives. TEFN has partially achieved state-of-the-art (SOTA) performance on various real-world datasets, with a notable reduction in training duration and model complexity when contrasted with Transformer-based models such as Crossformer [25] and Patch-based models like PatchTST [15]. In terms of random hyperparameter selection, TEFN demonstrates minimal variability, affirming its stability. The contributions of this manuscript are summarized as follows:

- The proposed method is well-suited for large datasets, showcasing exceptional performance.
- A novel evidential backbone BPA designed for extracting potential distributions from simple data structures is introduced.
- A BPA-based neural network, TEFN, is introduced for time series forecasting, outpacing prior research in terms of accuracy, efficiency, stability, and interpretability.
- The manuscript elucidates the incorporation of evidence theory concepts, such as the mass function, into the architecture of neural networks, offering a novel approach to uncertainty reasoning in machine learning.

This paper is organized as follows. We begin by reviewing relevant literature in the Section 2. Next, in the Section 3, we delve into the architecture and underlying mathematical principles of TEFN. In the Section 4, we present a series of experiments that demonstrate TEFN’s superior performance. Finally, we conclude the paper by summarizing our key findings in the Section 5.

2 RELATED WORK

2.1 Dempster-Shafer Theory

Dempster-Shafer theory, also known as Evidence Theory, operates on a different framework compared to traditional probability theory [6, 17]. It relies on the concept of mass functions, which provide a more flexible representation of uncertainty, accommodating weaker constraints than traditional probabilities. When combining two mass functions, denoted as m_1 and m_2 , the resulting fused mass function m is determined using the Dempster-Shafer Rule (DSR), as described in Equation 1. The symbols A , B , and C represent focal elements, which are typically combinations of all independent samples (or target labels, such as the classification targets).

$$m(A) = \sum_{B \cap C = A} m_1(B) * m_2(C) \quad (1)$$

2.2 Basic Probability Assignment

BPA is a core concept in evidence theory, used to map real data x into mass distributions. Mass distributions describe the degree of support for various hypotheses in the event space, providing a basis for reasoning and decision-making. The generation of BPA m is often based on fuzzy logic, where fuzzy membership functions μ are used to map data points to different fuzzy sets, thereby constructing the target distribution in Equation 2 where w and b is weight and bias of the membership function. BPA can also be generated

by assigning support degrees through Gaussian distributions N (probability density function f) where μ and σ are expectation and variance in Equation 3.

$$m = \mu(x) = wx + b \quad (2)$$

$$x \sim N(\mu, \sigma)$$

$$m = f(x) = \frac{1}{\sqrt{2\pi\sigma^2}} e^{-\frac{(x-\mu)^2}{2\sigma^2}} \quad (3)$$

The advantage of BPA lies in its ability to effectively handle uncertainty and improve the accuracy and reliability of predictions by fusing multi-source information.

2.3 Evidence Decision Making

The process of Evidence Decision Making can be delineated into several sequential steps: basic probability assignment (BPA), evidence fusion, and decision making (DM) [7, 23]. BPA serves as a pivotal initial phase, constituting a mapping from raw data to mass distribution, akin to the path from raw data to probability distribution. Subsequently, evidence fusion integrates distinct mass distributions from various data channels, culminating in a rationalized mass distribution. The most classic fusion method is the DSR [6, 17] mentioned in Section 2.1. Finally, decision making transpires as the progression from the attained distribution towards the designated target. The most classic decision-making method is to transform the mass distribution into the probability distribution of the target, called pignostic probability transformation (PPT) [9] in Equation 4, where x is a target label and e are combinations of all possible target labels.

$$p(x) = \sum_{e \in e} \frac{m(e)}{(1 - m(\emptyset)|e|)} \quad (4)$$

2.4 Linear Time Series Model

There are many linear time series forecasting models (LTSFM). LTSFM offer several advantages for modeling and forecasting time series data. Firstly, their simplicity and transparency make them easy to implement, interpret, and analyze. The parameters of linear models directly represent the relationships between input features and the output, providing insights into the underlying dynamics of the time series. Secondly, LTSFM exhibit high efficiency, requiring fewer computational resources and hyperparameters compared to complex models like transformer-based models [18, 25]. This leads to faster training and inference times, making them suitable for real-time applications and large datasets.

A classic LTSFM model is Dlinear [22]. DLinear serves as a simple yet effective baseline for long-term time series forecasting. It is a model that employs a seasonal-trend decomposition technique to separate the trend and seasonal components of the time series data. Each component is then independently modeled using a single-layer linear regression. The final prediction is obtained by summing the outputs of the two linear regressions.

TEFN shares similarities with Dlinear in that both models utilize linear regression for prediction. However, there are key differences:

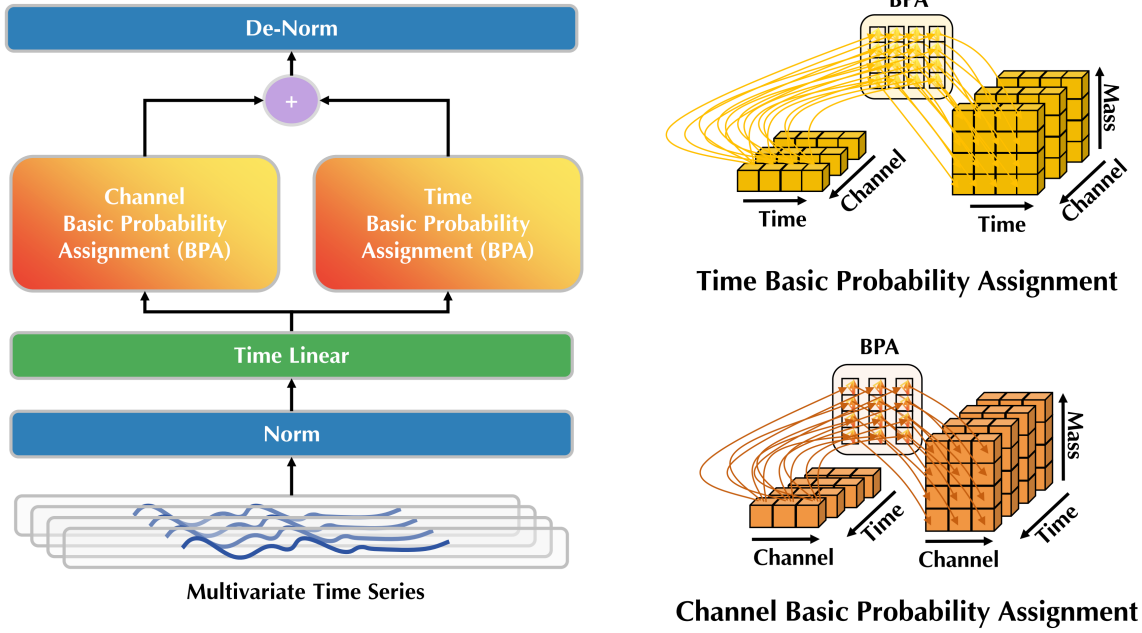


Figure 3: The overall structure of TEFN

- DLinear employs a simpler decomposition method compared to TEFN, which may limit its ability to capture intricate temporal dynamics.
- DLinear focuses on capturing linear relationships and trends in the data, while TEFN focuses on the mining of internal hidden relationships, so it strengthens predictions through dimensionality increase and uncertain reasoning.
- TEFN is a general framework that does not require identification and prediction of trends and periodicity, while DLinear is more like a feature modeling prediction of time series.

3 TIME EVIDENCE FUSION NETWORK

The structure of TEFN is inherently straightforward, achieving remarkable performance with a design featuring only two BPA modules, akin to employing just two convolutional kernels. We posit that the novel architecture of TEFN embodies the essence of a pure backbone model, stripped of domain-specific intricacies. This minimalist approach allows TEFN to focus solely on capturing the fundamental temporal patterns within the data, making it a versatile and adaptable foundation for various time series analysis tasks. The overall structure of TEFN is depicted in Figure 3.

3.1 Time Normalization and De-normalization

To expedite convergence towards local optima and enhance training efficiency, TEFN incorporates a normalization technique inspired by the Stationary model [14]. This process computes the mean μ

as shown in Equation 5 and variance σ^2 as shown in Equation 6 for each segment of the time series x . The subsequent normalization and de-normalization operations, presented in Equation 7 and Equation 8, respectively, act as symmetrical transformations that standardize the time series data. The neural network operation $Net(\cdot)$ is then applied to the normalized time series x_{Norm} , ensuring that the model learns from data with consistent scale and distribution. This normalization strategy effectively mitigates the influence of outliers and initial data scale, fostering faster convergence and improved stability during training.

$$\mu = \frac{1}{|x|} \sum_{x_i \in x} x_i \quad (5)$$

$$\sigma^2 = \frac{1}{|x|} \sum_{x_i \in x} (x_i - \mu)^2 = \frac{1}{|x|} \sum_{x_i \in x} x_i^2 - \mu^2 \quad (6)$$

$$x_{Norm} = \frac{x - \mu}{\sigma} \quad (7)$$

$$x_{De-Norm} = \sigma * \hat{y}_{Norm} + \mu = \sigma * Net(x_{Norm}) + \mu \quad (8)$$

3.2 Time Dimension Projection

In TEFN, we employ a linear layer $project(\cdot)$ to project dimensionality to an expansion dimensionality, transforming the input time series x with a length of L_{in} into a sequence x' with a length of $L_{in} + L_{pred}$ in Equation 9. Here, L_{pred} represents the desired length of the prediction horizon. This operation is analogous to

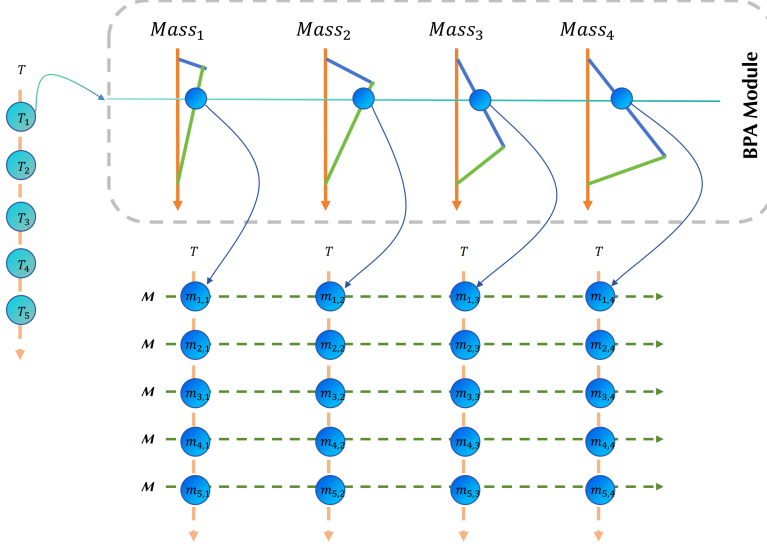


Figure 4: The operation process of a BPA module for a time series T of length $L = 5$. The sample space size in the BPA module is set as $|S| = 2$, and the event space size is set as $|2^S| = 2^{|S|} = 4$. The operation of the BPA module is similar to that of the convolution module, but the BPA module diffuses different masses instead of summing them in the convolution.

the time projection mechanism utilized in other neural network architectures, such as TimesNet [20].

$$x' = \text{project}(x) = x \times W_p + b \quad (9)$$

By extending the input vector to match the prediction length, the time projection layer facilitates the direct generation of future values based on the learned temporal patterns. This approach simplifies the model design and enables efficient prediction without the need for iterative or recursive computations, as commonly observed in autoregressive models.

3.3 Basic Probability Assignment Module

In TEFN, we leverage the principles of Evidence Theory to model the uncertainty and ambiguity inherent in time series data. According to Evidence Theory, each dimension of the time series can be represented as a mass function within a common event space. This event space is typically defined as the power set 2^S of the sample space S , where S represents the possible values or labels for the data. For classification problems, S corresponds to all the possible labels, while for regression problems, S is treated as a set of anonymous samples, ensuring mutual exclusivity among them.

This representation allows us to capture the fuzzy nature of the data, where each dimension generates a mass distribution within the event space. To achieve this, we utilize parameterized fuzzy membership functions, as defined in Equation 10. Here, D represents the dimensionality of the time series, encompassing both the time dimension T and the channel dimension C . The indices i and j correspond to the specific dimensions within D , while k represents the index of the event space dimension, denoted as F . The fuzzy membership function μ_k is defined in Equation 10 where $w_{D,j,k}$ and

$b_{D,j,k}$ are the slope and intercept parameters of the membership function, respectively. These parameters are learned during training and allow the model to capture the varying degrees of membership for each data point within the event space.

$$m_{D,i,j,k} = \mu(x_{\text{Norm},i,j}) = w_{D,j,k} * x_{\text{Norm},i,j} + b_{D,j,k} \quad (10)$$

By employing evidence theory and fuzzy membership functions, TEFN effectively models the uncertainty in time series data and enables the generation of robust and accurate predictions. This approach provides a principled way to handle the inherent fuzziness and ambiguity in real-world time series, leading to improved performance and reliability in various applications.

To introduce non-linear characteristics into TEFN and enhance its modeling capabilities, we can modify the fuzzy membership function used in the BPA module. Instead of the linear form presented in Equation 10, we can adopt non-linear functions that capture more complex relationships within the data. Several options exist for non-linear membership functions, including:

- **Gaussian Function:** This function models the data distribution as a bell-shaped curve such as Equation 3, capturing the likelihood of each data point belonging to different membership levels. The parameters of the Gaussian function can be learned to adapt to the specific characteristics of the time series data.
- **Sigmoid Function:** This function smoothly transitions between 0 and 1, providing a flexible way to represent the membership of data points to different levels in Equation 11. The sigmoid function can capture both gradual and abrupt changes in membership values.

$$\sigma(x) = \begin{cases} 0 & \text{if } x < 0 \\ \frac{1}{1+e^{-x}} & \text{if } x \geq 0 \end{cases} \quad (11)$$

- **Piecewise Functions:** These functions consist of multiple linear or non-linear segments, allowing for more precise control over the shape of the membership function in Equation 12 where $g(x)$ is a non-linear function. This approach is useful for capturing complex patterns and relationships within the data.

$$f(x) = \begin{cases} a_1x + b_1 & \text{if } c_1x + d_1 \leq 0 \\ g_1(x) & \text{if } c_2x + d_2 > 0 \text{ and } c_3x + d_3 \leq 0 \\ a_2x + b_2 & \text{if } c_4x + d_4 > 0 \\ \vdots \\ a_nx + b_n & \text{otherwise} \end{cases} \quad (12)$$

By utilizing non-linear membership functions, TEFN can effectively model the non-linear dynamics and interactions within the time series data. This enhancement enables TEFN to capture more subtle patterns and relationships, leading to improved accuracy and generalization in various time series forecasting tasks.

3.4 Expectation Fusion

TEFN addresses the challenge of handling multivariate time series data with two distinct dimensions: the time dimension T and the channel dimension C . This results in the paralleled generation of different mass distributions for each dimension, denoted as m_C and m_T . To integrate these mass distributions and produce a unified prediction, TEFN employs a fusion method based on expectations, as defined in Equation 13. Here, $y_{j,k}$ represents the fusion parameters, and $m'_{i,j,k}$ corresponds to the transformed mass function for each dimension.

$$\hat{y}_{Norm,D,i,j} = E_{D,F}(y_{j,k}) = \sum_{\substack{j \in [1,|D|] \\ k \in [1,|2^S|]}} y_{j,k} * m'_{i,j,k} = \sum_{\substack{j \in [1,|D|] \\ k \in [1,|2^S|]}} m_{i,j,k} \quad (13)$$

The fusion operation in Equation 13 can be interpreted as a linear transformation of the mass functions, where the summation of $y_{j,k} * m'_{i,j,k}$ effectively combines the information from different dimensions. The expectation is then calculated by summing the transformed mass functions, resulting in a single mass function representing the fused prediction.

TEFN deliberately avoids using the Dempster-Shafer Rule of Combination (DSR) for several reasons. Firstly, the computational complexity of DSR is significantly higher compared to the expectation-based fusion method. Additionally, DSR involves point-to-point multiplication of mass distributions within the same dimension, which can lead to accuracy loss when dealing with high-dimensional data due to finite precision limitations.

Secondly, DSR is sensitive to extreme distributions, particularly those with a single element having a value of 1. This sensitivity can result in the final fused result being dominated by that single distribution, potentially leading to conflicts and loss of information from other distributions.

By employing the expectation-based fusion method, TEFN achieves a balance between computational efficiency and accuracy. This approach effectively integrates information from different dimensions while mitigating the risks of conflicts and accuracy loss associated with DSR. The final normalized prediction results are then aggregated across dimensions using the equation in Equation 14 and restored to their original scale through the de-normalization layer.

$$\hat{y}_{norm} = \sum_{D \in \{T,C\}} \hat{y}_{Norm,D} = \hat{y}_{Norm,T} + \hat{y}_{Norm,C} \quad (14)$$

4 EXPERIMENTS

The experimental section aims to comprehensively evaluate TEFN's performance in long-term time series forecasting. Utilizing diverse datasets, TEFN will be benchmarked against established models, measuring accuracy, efficiency, and robustness. We will analyze its performance across different prediction horizons, assess its sensitivity to hyperparameters, and conduct ablation studies to understand the impact of individual components. Lastly, we will explore TEFN's interpretability by analyzing the basic probability assignments generated by its BPA module.

4.1 Dataset

Our research employs the TEFN for the challenging task of long-term time series prediction. To ensure the model's effectiveness and robustness across diverse scenarios, we meticulously selected five representative and extensively used datasets. These datasets encompass a wide range of real-world applications, providing a comprehensive evaluation of TEFN's performance. The selected datasets are:

- Electricity [1]: This dataset contains electricity load diagrams for a power grid from 2011 to 2014, offering insights into energy consumption patterns over time. It presents a challenging forecasting task due to its seasonal variations and potential anomalies.
- ETT (4 subsets) [11]: This dataset comprises four subsets with varying lengths and complexities, representing diverse time series forecasting challenges. It allows us to assess TEFN's ability to handle different data characteristics and prediction horizons.
- Exchange [21]: This dataset captures exchange rate fluctuations between major currencies. It presents a dynamic and volatile environment, testing TEFN's ability to capture complex market trends and predict future exchange rates accurately.
- Traffic [2]: This dataset contains traffic flow data collected from sensors in a city. It reflects the temporal and spatial patterns of traffic congestion, providing a challenging task for forecasting traffic flow and congestion levels.
- Weather [3]: This dataset includes historical weather data, encompassing various meteorological parameters. It allows us to evaluate TEFN's performance in predicting weather patterns, which are crucial for numerous applications like agriculture, disaster management, and transportation planning.

Each of these datasets is characterized by its large size and diverse features, offering a rich and challenging environment for evaluating TEFN’s capabilities. The extensive nature of the data ensures that the model is tested on a wide range of scenarios, providing valuable insights into its performance and generalizability. More dataset features are in the Table 1.

Table 1: The quantitative features of the dataset

Dataset	Dimension	Dataset Size
Electricity	321	(18317, 2633, 5261)
ETTm1, ETTm2	7	(34465, 11521, 11521)
ETTh1, ETTh2	7	(8545, 2881, 2881)
Traffic	862	(12185, 1757, 3509)
Weather	21	(36792, 5271, 10540)
Exchange	8	(5120, 665, 1422)

4.2 Comparative Baseline

To thoroughly evaluate the performance of the Time Evidence Fusion Network (TEFN), we compare it against a comprehensive set of state-of-the-art baseline models. These models represent various approaches and techniques commonly used in time series forecasting, providing a robust benchmark for assessing TEFN’s capabilities. The selected baseline models are as follows:

- Transformer-based Models:
 - iTransformer (ICLR 2024) [13]: A novel transformer architecture specifically designed for time series forecasting, showcasing the potential of transformer models in capturing long-range dependencies and complex temporal patterns.
 - PatchTST (ICLR 2023) [15]: This model divides the time series into patches and applies transformer-based operations on each patch independently. It demonstrates the effectiveness of patch-based approaches in reducing the computational complexity of transformer models while maintaining accuracy.
 - Crossformer (ICLR 2023) [25]: This model utilizes cross-attention mechanisms to capture interactions between different dimensions of time series data, demonstrating the effectiveness of transformer-based approaches in handling multivariate time series.
 - FEDformer (ICML 2022) [26]: A frequency-enhanced decomposed transformer model that captures both low-frequency and high-frequency components of time series data.
 - ETSformer [19]: A model that combines exponential smoothing and transformer-based approaches to capture both linear and non-linear trends in time series data.
 - Stationary (NeurIPS 2022) [14]: A model that utilizes a non-stationary transformer architecture to capture the evolving nature of time series data.

– Autoformer (NeurIPS 2021) [21]: A self-supervised transformer model that learns to forecast future values without relying on explicit labels. It leverages self-attention mechanisms to capture complex temporal patterns and relationships within the data.

- Linear Models:

- Rlinear (ICLR 2024) [12]: This model uses a single linear layer with reversible normalization (RevIN) to forecast time series data. It is effective at capturing periodic patterns and works well with longer input sequences.
- Dlinear (AAAI 2023) [22]: A linear model that employs seasonal-trend decomposition to capture the trend and seasonal components of time series data. It serves as a simple yet effective baseline for comparison.
- LightTS [24]: A lightweight model that utilizes a sampling-oriented MLP structure to achieve efficient and accurate time series forecasting.

- Other Models:

- TiDE (ICLR 2023) [5]: A time series dense encoder model that efficiently captures temporal patterns using a dense connection structure.
- TimeNet (ICLR 2023) [20]: A model that utilizes a temporal 2D-variation modeling approach to capture both time and frequency information in time series data.

By comparing TEFN against this diverse set of baseline models, we can comprehensively assess its performance and identify its unique advantages and contributions to the field of time series forecasting.

4.3 Implementation Details

Due to limited experimental equipment, our experimental environment was a regular desktop computer with a single CPU and a single GPU without paralleled computing of multi-GPU. Our experimental equipment is configured with AMD Ryzen9 7950x 4.5GHz 16 Cores , 64GB RAM DDR5 4800MHz, and NVIDIA RTX 4090 D 24GB. The proposed model TEFN is implemented in the PyTorch [16]. For the sake of fairness, we used an open-source benchmark located at <https://github.com/thuml/Time-Series-Library> which contains comparison models and corresponding experiment configurations. The open source address for our model is <https://github.com/ztxtech/Time-Evidence-Fusion-Network>. The loss function selected during the experiment was Mean Square Error (MSE), and the optimizer selected Adam [10]. We used Mean Absolute Error (MAE) and MSE in Equation 15 and Equation 16 as error indicators in the experiment where y_i is actual value and \hat{y}_i is predicted value.

$$MAE(y, \hat{y}) = \frac{1}{n} \sum_{i=1}^n |y_i - \hat{y}_i| \quad (15)$$

$$MSE(y, \hat{y}) = \frac{1}{n} \sum_{i=1}^n (y_i - \hat{y}_i)^2 \quad (16)$$

4.4 Forecasting Result

In the comparative experiment, we conducted a thorough comparison of 5 datasets and 12 comparative models in terms of forecasting length $L_{pred} \in \{96, 192, 336, 720\}$ in Table 2. The results

Table 2: This table presents a comprehensive comparison of prediction errors across various models for long-term time series forecasting tasks. The models are evaluated on four different prediction lengths: $L_{pred} \in \{96, 192, 336, 720\}$, providing a thorough assessment of their performance under varying forecasting horizons. The color coding in the table highlights the ranking of each model's performance across all datasets and prediction lengths, allowing for easy identification of the top-performing models.

Models	TEFN (Ours)	iTransformer [2023]	Rlinear [2023]	PatchTST [2023]	Crossformer [2023]	TiDE [2023]	TimesNet [2023]	ETSformer [2022]	LightTS [2022]	Dlinear [2023]	FEDformer [2022]	Stationary [2022]	Autoformer [2021]	
Metric	MSE	MAE	MSE	MAE	MSE	MAE	MSE	MAE	MSE	MAE	MSE	MAE	MSE	MAE
ETTm1	96	0.343 0.367 0.334 0.368	0.355 0.376 0.329 0.367	0.404 0.426 0.364 0.387	0.338 0.375 0.375 0.398	0.374 0.400 0.345 0.372	0.379 0.419 0.386 0.398	0.505 0.475						
	192	0.381 0.383 0.377 0.391	0.391 0.392 0.367 0.385	0.450 0.451 0.398 0.404	0.374 0.387 0.408 0.410	0.400 0.407 0.380 0.389	0.426 0.441 0.459 0.444	0.553 0.496						
	336	0.414 0.404 0.426 0.420	0.424 0.415 0.399 0.410	0.532 0.515 0.428 0.425	0.410 0.411 0.435 0.428	0.438 0.438 0.413 0.413	0.445 0.459 0.495 0.464	0.621 0.537						
	720	0.475 0.438 0.491 0.459	0.487 0.450 0.454 0.439	0.666 0.589 0.487 0.461	0.478 0.450 0.499 0.462	0.527 0.502 0.474 0.453	0.543 0.490 0.585 0.516	0.671 0.561						
	Avg	0.403 0.398 0.407 0.410	0.414 0.407 0.387 0.400	0.513 0.496 0.419 0.400 0.406	0.429 0.425 0.435 0.437	0.403 0.407 0.448 0.452	0.481 0.456 0.588 0.517							
ETTm2	96	0.181 0.264 0.180 0.264	0.182 0.265 0.175 0.259	0.287 0.366 0.207 0.305	0.187 0.267 0.189 0.280	0.209 0.308 0.193 0.292	0.203 0.287 0.192 0.274	0.255 0.339						
	192	0.246 0.304 0.250 0.309	0.246 0.304 0.241 0.302	0.414 0.492 0.290 0.364	0.249 0.309 0.253 0.319	0.311 0.382 0.284 0.362	0.269 0.328 0.280 0.339	0.281 0.340						
	336	0.307 0.343 0.311 0.348	0.307 0.342 0.305 0.343	0.597 0.542 0.377 0.422	0.321 0.351 0.314 0.357	0.442 0.466 0.369 0.427	0.325 0.366 0.334 0.361	0.339 0.372						
	720	0.407 0.398 0.412 0.407	0.407 0.398 0.402 0.400	1.730 1.042 0.558 0.524	0.408 0.403 0.414 0.413	0.675 0.587 0.554 0.522	0.421 0.415 0.417 0.413	0.433 0.432						
	Avg	0.286 0.327 0.288 0.332	0.286 0.327 0.281 0.326	0.757 0.610 0.358 0.404	0.291 0.333 0.293 0.342	0.409 0.436 0.350 0.401	0.305 0.349 0.306 0.347	0.327 0.371						
ETTh1	96	0.383 0.391 0.386 0.405	0.386 0.395 0.414 0.419	0.423 0.448 0.479 0.464	0.384 0.402 0.494 0.479	0.424 0.432 0.386 0.400	0.419 0.513 0.491 0.499	0.459 0.459						
	192	0.433 0.419 0.441 0.436	0.437 0.424 0.460 0.445	0.471 0.474 0.525 0.492	0.436 0.429 0.538 0.504	0.475 0.462 0.437 0.432	0.420 0.448 0.534 0.504	0.500 0.482						
	336	0.475 0.441 0.487 0.458	0.479 0.446 0.501 0.466	0.570 0.546 0.565 0.515	0.491 0.469 0.574 0.521	0.518 0.488 0.481 0.459	0.459 0.465 0.588 0.535	0.521 0.496						
	720	0.475 0.464 0.503 0.491	0.481 0.470 0.500 0.488	0.653 0.621 0.594 0.558	0.521 0.500 0.562 0.535	0.547 0.533 0.519 0.516	0.506 0.507 0.643 0.616	0.514 0.512						
	Avg	0.441 0.429 0.454 0.447	0.446 0.434 0.469 0.454	0.529 0.522 0.541 0.507	0.458 0.450 0.542 0.510	0.491 0.479 0.456 0.452	0.440 0.460 0.570 0.537	0.496 0.487						
ETTh2	96	0.288 0.337 0.297 0.349	0.288 0.338 0.302 0.348	0.745 0.584 0.400 0.440	0.340 0.374 0.340 0.391	0.397 0.437 0.333 0.387	0.358 0.397 0.476 0.458	0.346 0.388						
	192	0.375 0.392 0.380 0.400	0.374 0.390 0.388 0.400	0.877 0.656 0.528 0.509	0.402 0.414 0.430 0.439	0.520 0.504 0.477 0.476	0.429 0.439 0.512 0.493	0.456 0.452						
	336	0.423 0.434 0.428 0.432	0.415 0.426 0.426 0.433	1.043 0.731 0.643 0.571	0.452 0.452 0.485 0.479	0.626 0.559 0.594 0.541	0.496 0.487 0.552 0.551	0.482 0.486						
	720	0.434 0.446 0.427 0.445	0.420 0.440 0.431 0.446	1.104 0.763 0.874 0.679	0.462 0.468 0.500 0.497	0.863 0.672 0.831 0.657	0.463 0.474 0.562 0.560	0.515 0.511						
	Avg	0.380 0.402 0.383 0.407	0.374 0.398 0.387 0.407	0.942 0.684 0.611 0.550	0.414 0.427 0.439 0.452	0.602 0.543 0.559 0.515	0.437 0.449 0.526 0.516	0.450 0.459						
Electricity	96	0.197 0.273 0.148 0.240	0.201 0.281 0.181 0.270	0.219 0.314 0.237 0.329	0.168 0.272 0.187 0.304	0.207 0.307 0.197 0.282	0.193 0.308 0.169 0.273	0.201 0.317						
	192	0.197 0.276 0.162 0.253	0.201 0.283 0.188 0.274	0.231 0.322 0.236 0.330	0.184 0.289 0.199 0.315	0.213 0.316 0.196 0.285	0.201 0.315 0.182 0.286	0.222 0.334						
	336	0.212 0.292 0.178 0.269	0.215 0.298 0.204 0.293	0.246 0.337 0.249 0.344	0.198 0.300 0.212 0.329	0.230 0.333 0.209 0.301	0.214 0.329 0.200 0.304	0.231 0.338						
	720	0.253 0.325 0.225 0.317	0.257 0.331 0.246 0.324	0.280 0.363 0.284 0.373	0.220 0.320 0.233 0.345	0.265 0.360 0.245 0.333	0.246 0.355 0.222 0.321	0.254 0.361						
	Avg	0.215 0.292 0.178 0.270	0.219 0.298 0.205 0.290	0.244 0.334 0.251 0.344	0.192 0.295 0.208 0.323	0.229 0.329 0.212 0.300	0.214 0.327 0.193 0.296	0.227 0.338						
Exchange	96	0.082 0.198 0.086 0.206	0.093 0.217 0.088 0.205	0.256 0.367 0.094 0.218	0.107 0.234 0.085 0.204	0.116 0.262 0.088 0.218	0.148 0.278 0.111 0.237	0.197 0.323						
	192	0.176 0.297 0.177 0.299	0.184 0.307 0.176 0.299	0.470 0.509 0.184 0.307	0.226 0.344 0.182 0.303	0.215 0.359 0.176 0.315	0.271 0.380 0.219 0.335	0.300 0.369						
	336	0.328 0.412 0.331 0.417	0.351 0.432 0.301 0.397	1.268 0.883 0.349 0.431	0.367 0.448 0.348 0.428	0.377 0.466 0.313 0.427	0.460 0.500 0.421 0.476	0.509 0.524						
	720	0.861 0.700 0.847 0.691	0.886 0.714 0.901 0.714	1.767 1.068 0.852 0.698	0.964 0.746 1.025 0.774	0.831 0.699 0.839 0.695	1.195 0.841 1.092 0.769	1.447 0.941						
	Avg	0.362 0.402 0.360 0.403	0.378 0.417 0.367 0.404	0.940 0.707 0.370 0.413	0.416 0.443 0.410 0.427	0.385 0.447 0.354 0.414	0.519 0.500 0.461 0.454	0.613 0.539						
Traffic	96	0.645 0.383 0.395 0.268	0.649 0.389 0.462 0.295	0.522 0.290 0.805 0.493	0.593 0.321 0.607 0.392	0.615 0.391 0.650 0.396	0.587 0.366 0.612 0.338	0.613 0.388						
	192	0.598 0.360 0.417 0.276	0.601 0.366 0.466 0.296	0.530 0.293 0.756 0.474	0.617 0.336 0.621 0.399	0.601 0.382 0.598 0.370	0.604 0.373 0.613 0.340	0.616 0.382						
	336	0.605 0.362 0.433 0.283	0.609 0.369 0.482 0.304	0.558 0.305 0.762 0.477	0.629 0.336 0.622 0.396	0.613 0.386 0.605 0.373	0.621 0.383 0.618 0.328	0.622 0.337						
	720	0.644 0.382 0.467 0.302	0.647 0.387 0.514 0.322	0.589 0.328 0.719 0.449	0.640 0.350 0.632 0.396	0.658 0.407 0.645 0.394	0.626 0.382 0.653 0.355	0.660 0.408						
	Avg	0.623 0.372 0.428 0.282	0.626 0.378 0.481 0.304	0.550 0.304 0.760 0.473	0.620 0.336 0.621 0.396	0.622 0.392 0.625 0.383	0.610 0.376 0.624 0.340	0.628 0.379						
Weather	96	0.182 0.227 0.174 0.214	0.192 0.232 0.177 0.218	0.158 0.230 0.202 0.261	0.172 0.220 0.197 0.281	0.182 0.242 0.196 0.255	0.217 0.296 0.173 0.223	0.266 0.336						
	192	0.227 0.262 0.221 0.254	0.240 0.271 0.225 0.259	0.206 0.277 0.242 0.298	0.219 0.261 0.237 0.312	0.227 0.287 0.237 0.296	0.276 0.336 0.245 0.285	0.307 0.367						
	336	0.279 0.298 0.278 0.296	0.292 0.307 0.278 0.297	0.335 0.287 0.280 0.335	0.283 0.306 0.298 0.353	0.282 0.334 0.283 0.335	0.339 0.380 0.321 0.338	0.359 0.395						
	720	0.352 0.344 0.358 0.347	0.364 0.353 0.354 0.348	0.398 0.418 0.351 0.386	0.365 0.359 0.352 0.288	0.352 0.386 0.345 0.381	0.403 0.428 0.414 0.410	0.419 0.428						
	Avg	0.260 0.283 0.258 0.278	0.272 0.291 0.259 0.281	0.259 0.315 0.271 0.320	0.259 0.287 0.271 0.334	0.261 0.312 0.265 0.317	0.309 0.360 0.288 0.314	0.338 0.382						
1st Count	4	15												

Table 3: Full results of hyperparameter sensitivity

S	lr	Target	Dataset																															
			Electricity						ETTh1						ETTh2						ETTm1			ETTm2			Exchange			Traffic			Weather	
			MSE	MAE	MSE	MAE	MSE	MAE	MSE	MAE	MSE	MAE	MSE	MAE	MSE	MAE	MSE	MAE	MSE	MAE	MSE	MAE	MSE	MAE	MSE	MAE								
0	1 * 10 ⁻²	96	0.197	0.274	0.403	0.407	0.288	0.337	0.344	0.368	0.182	0.264	0.086	0.204	0.645	0.384	0.186	0.230	0.645	0.384	0.182	0.227	0.645	0.384	0.182	0.227								
		192	0.197	0.276	0.433	0.420	0.375	0.392	0.385	0.385	0.247	0.305	0.178	0.299	0.598	0.360	0.232	0.266	0.598	0.360	0.232	0.266	0.598	0.360	0.232	0.266								
		336	0.212	0.292	0.478	0.443	0.423	0.434	0.414	0.404	0.310	0.344	0.328	0.412	0.605	0.362	0.283	0.301	0.605	0.362	0.283	0.301	0.605	0.362	0.283	0.301								
	5 * 10 ⁻²	96	0.197	0.274	0.383	0.391	0.291	0.340	0.347	0.369	0.182	0.264	0.082	0.198	0.645	0.384	0.183	0.228	0.645	0.383	0.183	0.228	0.645	0.383	0.183	0.228								
		192	0.197	0.277	0.433	0.420	0.376	0.393	0.383	0.385	0.257	0.314	0.180	0.300	0.598	0.360	0.244	0.274	0.598	0.360	0.244	0.274	0.598	0.360	0.244	0.274								
		336	0.213	0.294	0.476	0.441	0.424	0.435	0.416	0.406	0.309	0.344	0.340	0.421	0.605	0.363	0.292	0.308	0.605	0.363	0.292	0.308	0.605	0.363	0.292	0.308								
1	1 * 10 ⁻¹	96	0.197	0.274	0.383	0.391	0.291	0.340	0.347	0.369	0.182	0.264	0.082	0.198	0.645	0.383	0.183	0.228	0.645	0.383	0.183	0.228	0.645	0.383	0.183	0.228								
		192	0.197	0.277	0.433	0.419	0.376	0.394	0.383	0.385	0.257	0.314	0.180	0.300	0.598	0.360	0.244	0.274	0.598	0.360	0.244	0.274	0.598	0.360	0.244	0.274								
		336	0.214	0.295	0.476	0.441	0.424	0.435	0.416	0.406	0.309	0.344	0.340	0.421	0.605	0.363	0.292	0.308	0.605	0.363	0.292	0.308	0.605	0.363	0.292	0.308								
	5 * 10 ⁻²	96	0.198	0.275	0.386	0.393	0.294	0.341	0.346	0.369	0.182	0.265	0.083	0.199	0.645	0.385	0.194	0.239	0.645	0.385	0.194	0.239	0.645	0.385	0.194	0.239								
		192	0.197	0.277	0.438	0.422	0.375	0.392	0.383	0.385	0.247	0.305	0.184	0.304	0.598	0.360	0.241	0.274	0.598	0.360	0.241	0.274	0.598	0.360	0.241	0.274								
		336	0.212	0.292	0.475	0.441	0.425	0.435	0.418	0.407	0.307	0.343	0.335	0.418	0.606	0.363	0.280	0.299	0.606	0.363	0.280	0.299	0.606	0.363	0.280	0.299								
2	1 * 10 ⁻²	96	0.197	0.274	0.384	0.392	0.289	0.337	0.349	0.369	0.182	0.265	0.083	0.205	0.645	0.383	0.202	0.249	0.645	0.383	0.202	0.249	0.645	0.383	0.202	0.249								
		192	0.197	0.276	0.434	0.420	0.375	0.393	0.386	0.388	0.247	0.305	0.177	0.298	0.598	0.360	0.232	0.266	0.598	0.360	0.232	0.266	0.598	0.360	0.232	0.266								
		336	0.212	0.292	0.476	0.441	0.423	0.435	0.414	0.405	0.311	0.346	0.348	0.427	0.605	0.363	0.284	0.301	0.605	0.363	0.284	0.301	0.605	0.363	0.284	0.301								
	5 * 10 ⁻²	96	0.197	0.274	0.383	0.391	0.289	0.338	0.345	0.368	0.182	0.265	0.084	0.202	0.646	0.384	0.183	0.228	0.646	0.384	0.183	0.228	0.646	0.384	0.183	0.228								
		192	0.197	0.277	0.434	0.420	0.377	0.394	0.384	0.387	0.247	0.305	0.177	0.298	0.598	0.360	0.228	0.263	0.598	0.360	0.228	0.263	0.598	0.360	0.228	0.263								
		336	0.212	0.292	0.477	0.443	0.424	0.436	0.415	0.405	0.308	0.343	0.353	0.430	0.605	0.363	0.293	0.309	0.605	0.363	0.293	0.309	0.605	0.363	0.293	0.309								
3	1 * 10 ⁻¹	96	0.197	0.274	0.384	0.391	0.289	0.339	0.347	0.368	0.182	0.265	0.088	0.205	0.646	0.385	0.186	0.231	0.646	0.385	0.186	0.231	0.646	0.385	0.186	0.231								
		192	0.197	0.277	0.438	0.423	0.378	0.395	0.387	0.387	0.247	0.305	0.191	0.310	0.598	0.361	0.241	0.278	0.598	0.361	0.241	0.278	0.598	0.361	0.241	0.278								
		336	0.212	0.293	0.480	0.446	0.425	0.437	0.416	0.406	0.308	0.343	0.343	0.463	0.605	0.363	0.299	0.316	0.605	0.363	0.299	0.316	0.605	0.363	0.299	0.316								
	5 * 10 ⁻²	96	0.197	0.274	0.384	0.391	0.291	0.339	0.347	0.368	0.182	0.265	0.088	0.205	0.646	0.385	0.187	0.230	0.646	0.385	0.187	0.230	0.646	0.385	0.187	0.230								
		192	0.197	0.276	0.434	0.420	0.376	0.393	0.383	0.385	0.248	0.305	0.177	0.298	0.598	0.360	0.232	0.266	0.598	0.360	0.232	0.266	0.598	0.360	0.232	0.266								
		336	0.213	0.293	0.477	0.443	0.424	0.436	0.415	0.406	0.308	0.343	0.353	0.429	0.606	0.363	0.285	0.303	0.606	0.363	0.285	0.303	0.606	0.363	0.285	0.303								
4	1 * 10 ⁻²	96	0.197	0.274	0.384	0.391	0.291	0.339	0.346	0.368	0.184	0.266	0.084	0.201	0.645	0.384	0.196	0.245	0.645	0.384	0.196	0.245	0.645	0.384	0.196	0.245								
		192	0.197	0.277	0.434	0.420	0.377	0.394	0.385	0.386	0.248	0.306	0.176	0.297	0.598	0.360	0.254	0.280	0.598	0.360	0.254	0.280	0.598	0.360	0.254	0.280								
		336	0.212	0.293	0.477	0.443	0.424	0.436	0.415	0.406	0.308	0.343	0.353	0.435	0.607	0.363	0.288	0.308	0.607	0.363	0.288	0.308	0.607	0.363	0.288	0.308								
	5 * 10 ⁻²	96	0.197	0.274	0.383	0.392	0.292	0.340	0.345	0.368	0.181	0.264	0.085	0.203	0.645	0.384	0.197	0.234	0.645	0.384	0.197	0.234	0.645	0.384	0.197	0.234								
		192	0.198	0.278	0.433	0.420	0.377	0.394	0.385	0.386	0.248	0.307	0.179	0.300	0.598	0.360	0.234	0.270	0.598	0.360	0.234	0.270	0.598	0.360	0.234	0.270								
		336	0.212	0.292	0.475	0.441	0.422	0.434	0.416	0.407	0.312	0.347	0.346	0.427	0.607	0.363	0.288	0.307	0.607	0.363	0.288	0.307	0.607	0.363	0.288	0.307								
5	1 * 10 ⁻²	96	0.198	0.275	0.384	0.391	0.291	0.340	0.347	0.368	0.182	0.265	0.083	0.201	0.646	0.385	0.184	0.229	0.646	0.385	0.184	0.229	0.646	0.385	0.184	0.229								
		192	0.198	0.277	0.434	0.421	0.379	0.396	0.381	0.385	0.247	0.305	0.187	0.306	0.600	0.362	0.227	0.262	0.600	0.362	0.227	0.262	0.600	0.362	0.227	0.262								
		336	0.212	0.293	0.475	0.441	0.422	0.434	0.416	0.406	0.308	0.343	0.340	0.421	0.606	0.363	0.280	0.309	0.606	0.363	0.280	0.309	0.606	0.363	0.280	0.309								
	5 * 10 ⁻²	96	0.198	0.274	0.383	0.391	0.291	0.340	0.347	0.368	0.183	0.265	0.085	0.204	0.645	0.386	0.185	0.230	0.645	0.386	0.185	0.230	0.645	0.386	0.185	0.230								
		192	0.198	0.278	0.433	0.419	0.378	0.395	0.382	0.383	0.248	0.306	0.177	0.299	0.599	0.362	0.251	0.288	0.599	0.362	0.251	0.288	0.599	0.362	0.251	0.288								
		336	0.212	0.292	0.475	0.441	0.422	0.434	0.418	0.407	0.313	0.348	0.347	0.427	0.607	0.363	0.280	0.307	0.607	0.363	0.280	0.307	0.607	0.363	0.280	0.307								
6	1 * 10 ⁻²	96	0.199	0.276	0.384	0.392	0.290	0.340	0.347	0.368	0.183	0.265																						

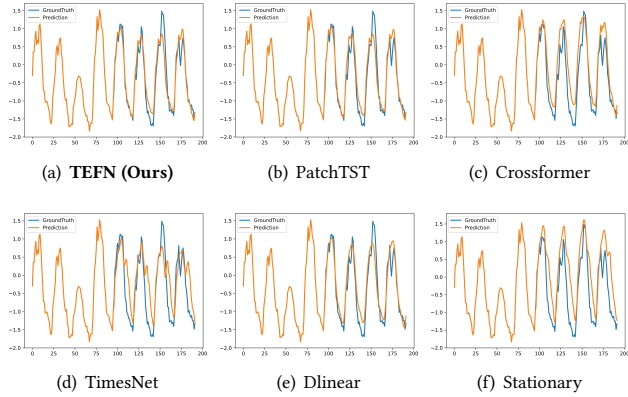


Figure 5: Visualization of Electricity-96 tasks

models. We take the task of Electricity-96 [1] as an example and selected typical models PatchTST [15], Crossformer [25], TimesNet [20], Dlinear [22] and Stationary [14] for visualization in Figure 5. From the visualization results, TEFN fits the details and trends of time series better.

4.5 Hyperparameter Sensitivity

To test the hyperparameter sensitivity of TEFN, we conducted a 2D traversal of the learning rate $lr \in \{10^{-2}, 5 * 10^{-2}, 10^{-1}\}$ and sample space size $|S| \in \{0, 1, 2, 3, 4, 5, 6\}$. We take the Electricity-96 task as an example. TEFN demonstrates weak sensitivity to parameters, but as the sample space increases, the error magnitude also increases, leading to a certain degree of overfitting in the model as shown in Figure 6. It is worth noting that the order of magnitude of the MSE in Figure 6 is 10^{-4} , while the order of magnitude of the compared MSE is 10^{-3} , so the fluctuation of different hyperparameter in error metrics is small. Full hyperparameter sensitivity experiment results are in the Table 3.

Additionally, we conducted statistical analysis on the error variance of different tasks as shown in Table 4. The order of magnitude of variance is 10^{-4} , indicating extremely small fluctuation. Random parameter selection within the traversal range of TEFN yields stable prediction results.

Table 4: The variance of model error for traversal learning rate and sample space

Metric (Var)	Dataset							
	Electricity	ETTh1	ETTh2	ETTm1	ETTm2	Exchange	Traffic	Weather
MSE	96	0.0000	0.0000	0.0002	0.0002	0.0001	0.0000	0.0001
	192	0.0001	0.0000	0.0003	0.0004	0.0000	0.0000	0.0002
	336	0.0001	0.0000	0.0002	0.0004	0.0000	0.0023	0.0000
	720	0.0000	0.0000	0.0004	0.0001	0.0000	0.0038	0.0001
MAE	96	0.0000	0.0000	0.0001	0.0001	0.0001	0.0000	0.0002
	192	0.0001	0.0000	0.0001	0.0001	0.0000	0.0000	0.0002
	336	0.0001	0.0000	0.0001	0.0001	0.0000	0.0009	0.0000
	720	0.0000	0.0000	0.0001	0.0000	0.0000	0.0007	0.0000

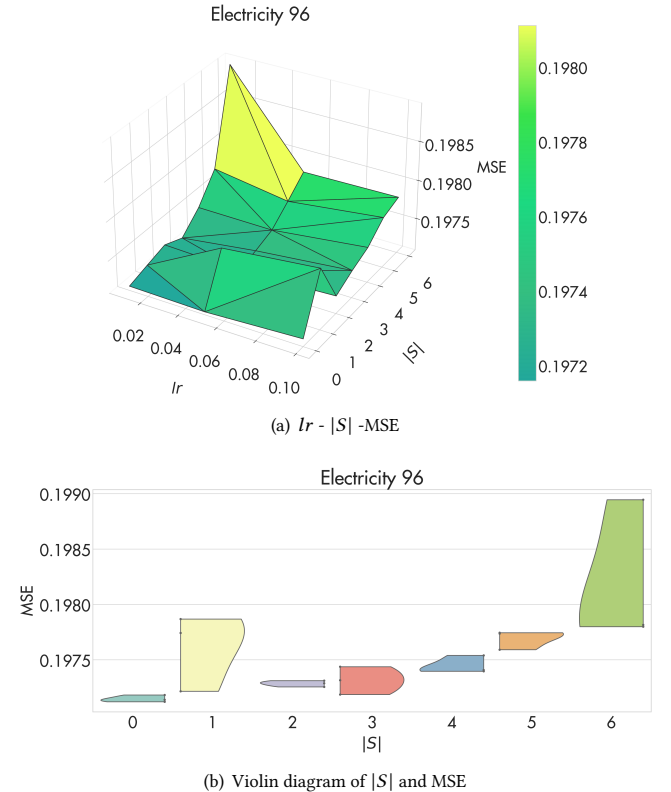


Figure 6: Traversing error of Electricity 96 task: 3D visualization and violin diagram. The points on the number axis of the violin chart reflect the density of learning rate.

4.6 Ablation Study

TEFN is formed by the fusion of time information sources T and channel information sources C . In the ablation experiment, we made separate predictions for the time and channel parts of TEFN as shown in Table 5. Across most forecasting tasks, the fusion $C + T$ error is lower than that of individual time T or channel C error. Although partial use of a single channel may further reduce prediction error, the error reduction is not significant (error of Electricity only varies 0.001). It displays that TEFN effectively filters out time T and channel C information, and individual time T and channel C information alone cannot effectively construct the evolution pattern of time series.

We conducted ablation experiments on all forecasting tasks, testing individual channel C forecasting and individual time T forecasting. We tested the forecasting length $L_{pred} \in \{96, 192, 336, 720\}$ and averaged Avg the errors of the four forecasting lengths in Table 5. In the aspect of all the results of ablation, TEFN can effectively improve the performance by combining the dimensions of time T and channel C in most cases. There are a few cases where the effect is not as good as the individual dimensions, but the difference is small and can be ignored. According to the characteristics of neural networks, the forecasting error of TEFN l_{C+T} will be less than or equal to using separate time l_T or channel l_C in Equation 17.

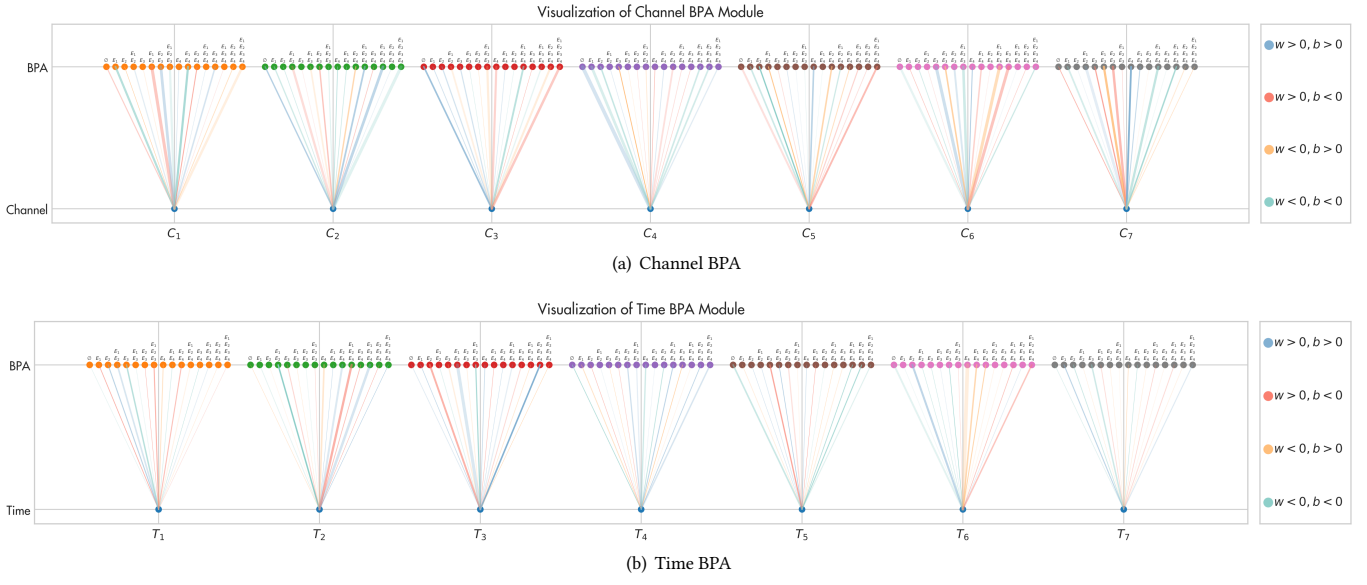


Figure 7: Visualization of Time BPA and Channel BPA modules in target ETTh1-96: Each line represents the fuzzy set membership function corresponding to the time. The fuzzy numbers established in TEFN are all triangular fuzzy numbers, and different channels C_i and time T_i can correspond to fuzzy sets that conform to symbolic logic.

Table 5: The results of the ablation experiment

Metric	Target	Model	Dataset							
			Electricity	ETTh1	ETTh2	ETTm1	ETTm2	Exchange	Traffic	Weather
MSE	96	C+T	0.197	0.383	0.288	0.343	0.181	0.082	0.645	0.182
		C	0.196↓	0.386↑	0.288	0.339↓	0.185↑	0.083↑	0.644↓	0.185↑
		T	0.197	0.291↑	0.356↑	0.182↑	0.083↑	0.645	0.195↑	
MSE	192	C+T	0.197	0.433	0.375	0.381	0.246	0.176	0.598	0.227
		C	0.196↓	0.435↑	0.375	0.382↑	0.246	0.179↑	0.597↓	0.230↑
		T	0.197	0.435↑	0.375	0.390↑	0.247↑	0.175↓	0.598	0.240↑
MSE	336	C+T	0.212	0.475	0.423	0.414	0.307	0.328	0.605	0.279
		C	0.210↓	0.479↑	0.423	0.411↓	0.307	0.336↑	0.604↑	0.280↑
		T	0.212	0.479↑	0.414↓	0.423↑	0.307	0.324↓	0.606↑	0.291↑
MSE	720	C+T	0.253	0.475	0.434	0.475	0.407	0.861	0.644	0.352
		C	0.253	0.478↑	0.457↑	0.472↓	0.407	0.947↑	0.642↓	0.354↑
		T	0.254↑	0.479↑	0.442↑	0.487↑	0.408↑	0.871↑	0.643↓	0.364↑
Avg	Avg	C+T	0.215	0.441	0.380	0.403	0.286	0.362	0.623	0.260
		C	0.214↓	0.444↑	0.386↑	0.401↓	0.286	0.386↑	0.622↓	0.262↑
		T	0.215	0.445↑	0.380	0.414↑	0.286	0.363↑	0.623	0.273↑
MAE	96	C+T	0.274	0.391	0.338	0.367	0.264	0.198	0.384	0.227
		C	0.273↓	0.394↑	0.339↑	0.366↓	0.269↑	0.199↑	0.384	0.228↑
		T	0.274	0.393↑	0.339↑	0.377↑	0.265↑	0.199↑	0.383↓	0.234↑
MAE	192	C+T	0.276	0.420	0.392	0.384	0.304	0.297	0.360	0.262
		C	0.275↓	0.421↑	0.393↑	0.385↑	0.305↑	0.300↑	0.361↑	0.264↑
		T	0.276	0.421↑	0.390↓	0.392↑	0.305↑	0.296↓	0.361↑	0.270↑
MAE	336	C+T	0.292	0.441	0.435	0.405	0.343	0.412	0.363	0.298
		C	0.291↓	0.443↑	0.434↓	0.403↓	0.343	0.419↑	0.363	0.298
		T	0.292	0.445↑	0.425↓	0.413↑	0.342↓	0.410↓	0.362↓	0.306↑
MAE	720	C+T	0.325	0.465	0.446	0.438	0.399	0.700	0.382	0.344
		C	0.325	0.463↓	0.462↑	0.436↓	0.399	0.739↑	0.382	0.347↑
		T	0.324↓	0.469↑	0.454↑	0.449↑	0.398↓	0.702↑	0.382	0.354↑
MAE	Avg	C+T	0.292	0.429	0.403	0.398	0.327	0.402	0.372	0.283
		C	0.291↓	0.430↑	0.407↑	0.397↓	0.329↑	0.414↑	0.373↑	0.284↑
		T	0.292	0.432↑	0.402↓	0.408↑	0.328↑	0.402	0.372	0.291↑

↑: Larger Error than C+T ↓: Smaller Error than C+T

$$l_{C+T} \leq \min(l_C, l_T) \quad (17)$$

4.7 Efficiency Comparison

TEFN is a compact model compared to the parameters of the Transformer. In order to effectively compare the efficiency of the model, we chose the dataset Electricity with a large dataset for performance comparison. In the task Electricity-96, we measured the average time, MSE, and exported model file size for iterating over one sample. Different models occupy varying amounts of GPU and memory. Therefore, we used the size of the saved binary model files as the model size. We visualized this with a bubble chart in Figure 8. It can be seen that TEFN achieves a low prediction error with an extremely small number of parameters. Meanwhile, it has the shortest average time for iterating over one sample, demonstrating its high efficiency. TEFN maintains almost Dlinear [22] performance and almost PatchTST [15] accuracy, making it a performance error balanced model.

It is particularly relevant to note that TEFN has demonstrated strong performance on portable devices. As evidenced by the official code repository (<https://github.com/ztxtech/Time-Evidence-Fusion-Network>), TEFN’s training and prediction processes have been successfully executed on a Macbook Air 2020 equipped with Apple Silicon M1 and 8GB RAM. This finding suggests that TEFN’s computational efficiency is well-suited for resource-constrained environments, contrasting with the challenges typically encountered by Transformer-based models such as Crossformer [25] when deployed on portable computers.

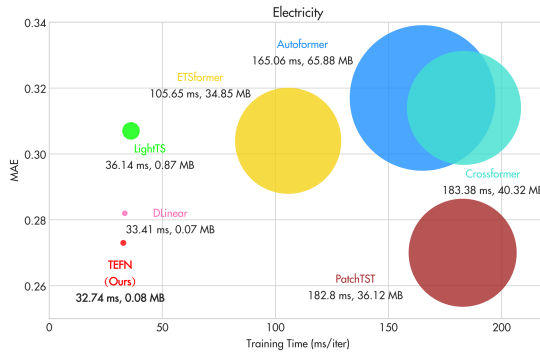


Figure 8: Model efficiency comparison. Results are from the prediction task Electricity-96, where the model size refers to the size of the binary model files, and iteration time is averaged each iterations.

4.8 Interpretability Analysis

The Time Evidence Fusion Network (TEFN) incorporates fuzzy logic and the Dempster-Shafer theory to effectively model the inherent uncertainty and ambiguity within time series data, resulting in a model that is not only accurate but also highly interpretable. TEFN allocates mass to events within the event space $E = \{E_i | i \in [1, 2^{|S|}]\}$, where each event represents a potential outcome or scenario. The mass assigned to an event reflects the level of confidence or support for that event, providing insight into the model’s belief about its likelihood of occurrence. This support allocation is particularly interpretable due to the use of fuzzy membership functions $\mu(x) = wx + b$ within the BPA module, as depicted in Figure 7. By analyzing the shape and parameters of these membership functions, users can gain a clear understanding of the model’s perception of data features and their influence on predictions. For instance, it becomes evident which features are deemed more important than others, and how the model responds to variations within these features. This visualization not only makes the model’s inner workings more transparent but also allows users to intuitively assess the model’s confidence in its predictions and the level of uncertainty associated with each outcome.

In summary, TEFN’s interpretability stems from its foundational reliance on fuzzy logic and the Dempster-Shafer theory, coupled with the transparency of its BPA and fuzzy reasoning processes. By exploring these aspects, users can develop a comprehensive understanding of the model’s decision-making process and prediction outcomes, fostering trust and confidence in the model’s capabilities.

4.9 Limitation and Future Prospects

TEFN is a naive and unmodified model. We lack skills in the application of BPA modules, such as how to generate BPA, and fuzzy logic is not the optimal implementation method. Due to fuzzy logic, TEFN is essentially a linear model that cannot handle some non-linear time series well. In addition, for the fusion of mass distribution in the face of the failure of the classic Dempster Shafer rule for a large amount of data, using expectations as the fusion method may

not necessarily be the optimal pattern. In terms of performance optimization, TEFN adopts a simple fully connected approach, which can lead to a rapid increase in parameter count for time series that are too long or have multiple channels. In fact, the implementation techniques of TEFN can further optimize the performance of the model through sampling and kernel operations similar to convolution. Thanks to the fact that evidence theory belongs to symbolic logic, the interpretation of neural network parameters will be more in line with human logic. Effective parameter initialization may exist, for example, initializing corresponding parameters in a non neural network way may lead to faster convergence.

5 CONCLUSION

This paper introduces the TEFN, a novel approach for long-term time series forecasting that is particularly well-suited for handling very large datasets. TEFN treats different channels and time points as distinct information sources, using evidence theory to construct basic probability assignments and discard irrelevant data. This selective information fusion significantly reduces the computational burden, enabling TEFN to efficiently process and predict within acceptable time frames. The model’s parameter efficiency, robustness, and interpretability make it a valuable tool for time series forecasting tasks involving large and complex datasets.

ACKNOWLEDGMENTS

The work is partially supported by National Natural Science Foundation of China (Grant No. 62373078)

REFERENCES

- [1] [n.d.]. Electricity Load Time Series Dataset. <https://archive.ics.uci.edu/ml/datasets/ElectricityLoadDiagrams20112014/>.
- [2] [n.d.]. Traffic Dataset. <http://pems.dot.ca.gov/>.
- [3] [n.d.]. Weather Dataset. <https://www.bgc-jena.mpg.de/wetter/>.
- [4] Yoshua Bengio, Yann LeCun, and Donnie Henderson. 1993. Globally trained handwritten word recognizer using spatial representation, convolutional neural networks, and hidden Markov models. *Advances in neural information processing systems* 6 (1993).
- [5] Abhimanyu Das, Weihao Kong, Andrew Leach, Rajat Sen, and Rose Yu. 2023. Long-term Forecasting with TiDE: Time-series Dense Encoder. *arXiv preprint arXiv:2304.08424* (2023).
- [6] AP DEMPSTER. 1967. Upper and Lower Probabilities Induced By A Multivalued Mapping. *Annals of Mathematical Statistics* 38 (1967), 325–339.
- [7] Yong Deng. 2015. Generalized evidence theory. *Applied Intelligence* 43, 3 (2015), 530–543.
- [8] Thierry Denoeux. 2000. A neural network classifier based on Dempster-Shafer theory. *IEEE Transactions on Systems, Man, and Cybernetics-Part A: Systems and Humans* 30, 2 (2000), 131–150.
- [9] Didier Dubois, Henri Prade, and Sandra Sandri. 1993. On possibility/probability transformations. In *Fuzzy logic: State of the art*. Springer, 103–112.
- [10] Diederik P. Kingma and Jimmy Ba. 2015. Adam: A Method for Stochastic Optimization. *ICLR* (2015).
- [11] Jianxin Li, Xiong Hui, and Wancai Zhang. 2021. Informer: Beyond efficient transformer for long sequence time-series forecasting. *arXiv:2012.07436* (2021).
- [12] Zhe Li, Shiyi Qi, Yiduo Li, and Zenglin Xu. 2023. Revisiting Long-term Time Series Forecasting: An Investigation on Linear Mapping. *arXiv preprint arXiv:2305.10721* (2023).
- [13] Yong Liu, Tengge Hu, Haoran Zhang, Haixu Wu, Shiyu Wang, Lintao Ma, and Mingsheng Long. 2023. itransformer: Inverted transformers are effective for time series forecasting. *ICLR* (2023).
- [14] Yong Liu, Haixu Wu, Jianmin Wang, and Mingsheng Long. 2022. Non-stationary Transformers: Rethinking the Stationarity in Time Series Forecasting. *NeurIPS* (2022).
- [15] Yuqi Nie, Nam H Nguyen, Phanwadee Sinthong, and Jayant Kalagnanam. 2023. A Time Series is Worth 64 Words: Long-term Forecasting with Transformers. *ICLR* (2023).

[16] Adam Paszke, S. Gross, Francisco Massa, A. Lerer, James Bradbury, Gregory Chanan, Trevor Killeen, Z. Lin, N. Gimelshein, L. Antiga, Alban Desmaison, Andreas Köpf, Edward Yang, Zach DeVito, Martin Raison, Alykhan Tejani, Sasank Chilamkurthy, Benoit Steiner, Lu Fang, Junjie Bai, and Soumith Chintala. 2019. PyTorch: An Imperative Style, High-Performance Deep Learning Library. *NeurIPS* (2019).

[17] Glenn Shafer. 1976. *A mathematical theory of evidence*. Vol. 42. Princeton university press.

[18] Ashish Vaswani. 2017. Attention is all you need. *arXiv preprint arXiv:1706.03762* (2017).

[19] Gerald Woo, Chenghao Liu, Doyen Sahoo, Akshat Kumar, and Steven C. H. Hoi. 2022. ETSformer: Exponential Smoothing Transformers for Time-series Forecasting. *arXiv preprint arXiv:2202.01381* (2022).

[20] Haixu Wu, Tengge Hu, Yong Liu, Hang Zhou, Jianmin Wang, and Mingsheng Long. 2023. TimesNet: Temporal 2D-Variation Modeling for General Time Series Analysis. *ICLR* (2023).

[21] Haixu Wu, Jiehui Xu, Jianmin Wang, and Mingsheng Long. 2021. Autoformer: Decomposition Transformers with Auto-Correlation for Long-Term Series Forecasting. *NeurIPS* (2021).

[22] Ailing Zeng, Muxi Chen, Lei Zhang, and Qiang Xu. 2023. Are Transformers Effective for Time Series Forecasting? *AAAI* (2023).

[23] Tianxiang Zhan, Zhen Li, and Yong Deng. 2024. Random Graph Set and Evidence Pattern Reasoning Model. *arXiv preprint arXiv:2402.13058* (2024).

[24] Tianping Zhang, Yizhuo Zhang, Wei Cao, Jiang Bian, Xiaohan Yi, Shun Zheng, and Jian Li. 2022. Less is more: Fast multivariate time series forecasting with light sampling-oriented mlp structures. *arXiv preprint arXiv:2207.01186* (2022).

[25] Yunhao Zhang and Junchi Yan. 2023. Crossformer: Transformer utilizing cross-dimension dependency for multivariate time series forecasting. *ICLR* (2023).

[26] Tian Zhou, Ziqing Ma, Qingsong Wen, Xue Wang, Liang Sun, and Rong Jin. 2022. FEDformer: Frequency enhanced decomposed transformer for long-term series forecasting. *ICML* (2022).